Aerodynamics of a wing body with different Winglet Cant Angle

Mit Piyush Bakhai[1], Shabudin Bin Mat[1], Nur Amalina Binti Musa[2]

[1]UTM Aerolab,Institute for Vehicle Systems and Engineering (IVeSE) School of Mechanical Engineering, Faculty of Engineering Universiti Teknologi Malaysia 81310 UTM Johor Bahru Johor, Malaysia
[2]Faculty of Engineering, City University Malaysia, Menara City U, No. 8, Jalan 51A/223, 46100 Petaling Jaya, Selangor.

*Corresponding Author: bit2017@gmail.com

Abstract. Current aircraft was designed with winglet at the tip. Winglets reduce the drag and improve fuel efficiency and range. The winglets have been in use for nearly 90 years, but it have been remained fixed. This paper presents the effects of winglet Cant angle on the aerodynamic characteristics of the wing. Winglet Cant Angle (WCA) is the angle between the vertical exis and the winglet. Computational Fluid Dynamics (CFD) has been used to simulate the Cant angles at constant angle of attack of 0º. In this paper the Cant angle was varied from 105º, 88º, 75º, 60º, 50º, 45º, 35º and the simulation works were performed at three different Flight levels of Sea level, 10000 and 15000 meters. The analysis analysis at 100 m/s velocity shows that Cant angle of 45º is the best performing Winglet while Cant 60º is the lowest performance in overall lift to drag Ratio. Similar results were obtained when Turbulent Kinematic Viscosity were measured at 20 m behind the wing. Flow visualization also showed the similar results Cant angle 45^0 is the best performance compared to other angles. For the best performing winglet, the lift to drag Ratio was lowest for perpendicular crosswinds. This study shows the effect of only winglet cant angle, however other factors involved to impact the performance of winglet are, Winglet height, winglet sweep angle, Winglet Cant angle, Winglet Toe angle, and crosswinds. To implement the best overall drag coefficient winglet, the optimization must be done mid-air. While calculating the parameters, the best most optimized winglet can be chosen for cruising flight level.

Keywords: Winglet, Winglet Cant Angle, Kinematic Turbulent Viscosity, Flow Visualization, Crosswind.

1 Introduction

The wing because of its airfoil characteristics will generate a pressure difference on the top and the bottom of the body which leads to lifting the of the airplane. Due to this abnormalityin pressure, on the upper and lower wing, at the tip of the wings the swirls starts to form, which are called as vortex, vortex are dangerous in airline industry and if a small aircraft comes in the contact with wake of a big aircraft, because of the very high gusts, it may stalltoo. As an example, a chartered aircraft with five people on board, including In-N-Out Burger's president, Rich Snyder, crashed several miles before John Wayne Airport in Orange County, California. The aircraft was following a Boeing 757 for landing, became caught in its wake turbulence, rolled into a deep descent and crashed. As a result of this and other incidents involving aircraft following behind a Boeing 757, the FAA now employs the separation rules of heavy aircraft for the Boeing 757 [1]. The solution to this problem is winglets which are also called as wingtip devices which are the small extension to the wing at the tip of the wing, which are generally angled upwards to reduce the effects of wake vortex and thus to increase the overall lift and reduce the drag coefficient. In the late 1970's R.T. Whitcomb, who developed the Modern style Winglet and considerably reducedthe Drag and improved the aircraft performance by up to 20% in terms of Lift induced Drag [2-4]. Winglets come in many shapes and sizes which include Whitcomb Style Winglet, Tip Fence Winglet, cantedwinglet, , Blended Winglet and many more, Most used winglet style is the Blended Winglet and the Whitcomb Style Winglet but most of them are fixed in nature if the winglets do change the Winglet Cant Angle midflight then the best Lift to Drag Ratio can be taken into consideration and the flight can continue flying its journey at the same angle throughout its entire journey.

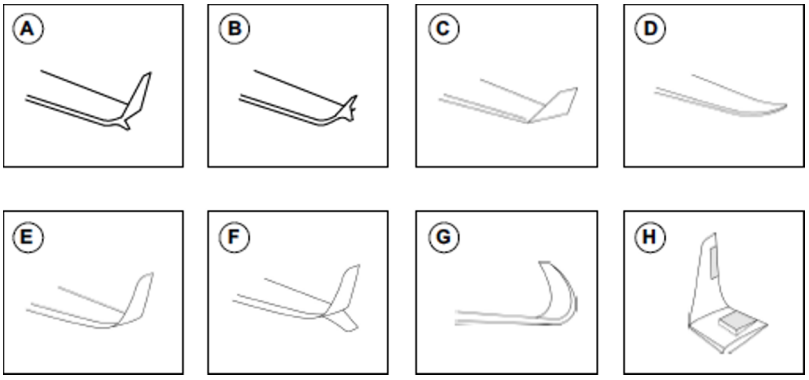

Fig. 1. Types of Winglets (A) Whitcomb winglet;(B) Tip fence; (C) Canted winglet; (D) Raked wingtip; (E) Blended winglet; (F) Blended split winglet; (G) Sharklet; (H) Active winglets.[3]

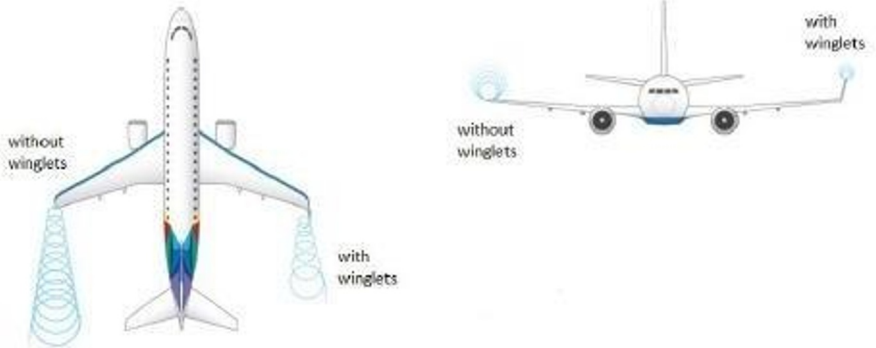

Fig. 2. Rough Illustration of the impact of Winglets in terms of Wake Vortex [4]

The current study deals with the NACA 4412 airfoil-based wing with the winglet Cant Angle of 35°, 45°, 50°, 60°, 75°, 88° and 105°. The CFD simulation is done through Open foam-based Simulation software called as Simscale. The Entire Simulation is done at the three different heights, sea level, ten thousand meters and fifteen thousand meters respectively. The Crosswind Analysis is also done on the 45° and 60° Winglet Cant Angle.

2 Methodology

2.1 Geometrical Modelling

The figure 3 shows the Winglet Cant Angle together with their wing bodystructure. Themodel was developed with the Solidworks Academic Version 2021.

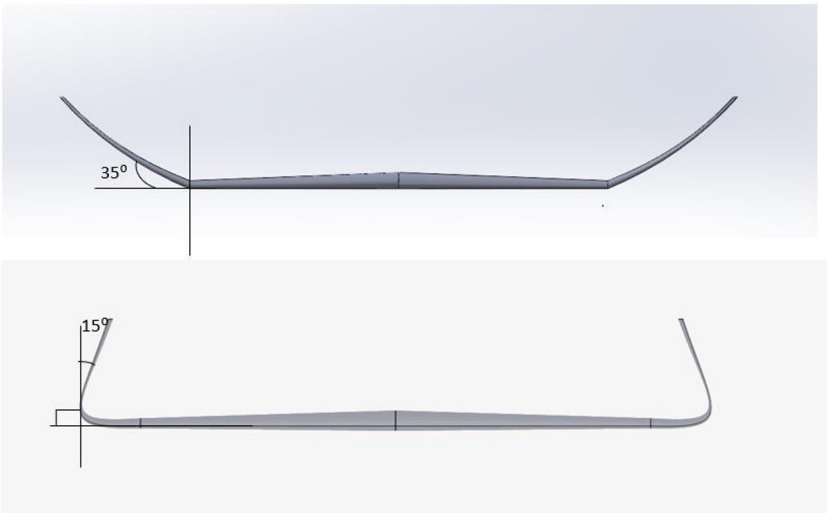

Fig. 3. Winglet with Cant angle of 35º and 105º respectively on top and bottom

The concept of Smart Homes has been gaining popularity in recent years, with the potential to improve energy efficiency and reduce costs for homeowners. One of the key challenges in Smart Home technology is optimizing energy utilization, which can be achieved through the use of machine learning techniques. Machine learning techniques have been proposed as a promising solution to the energy consumption optimization challenges. Machine learning techniques can learn from historical energy consumption data [5].

Here for the study angle of 88º is chosen as the last case for acute cant angle because, 90º creates a geometry which the simulation cannot do the simulation for, thus, to obtain the results near 90º we can nearly assume the flow field around 88º. Airfoil used in the construction of wings and winglet for all cases is NACA-4412i. Total wingspan excluding the winglet is 20 meters, chord length is 3.25 meters, and the height of the winglet is 4 meters(Figure 5), and the bodies are symmetric across the dotted green line as shown in figure 6 for all the cases with different cant angle.

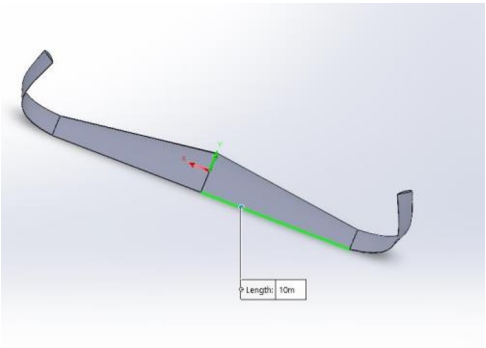

Fig. 4. The Wingspan Length

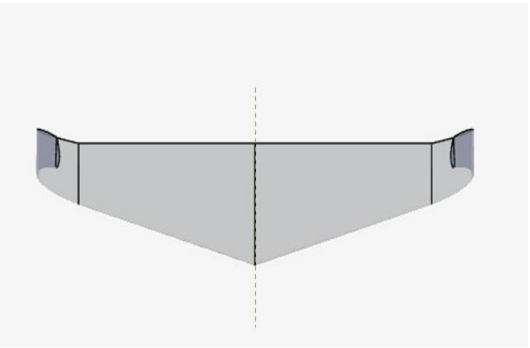

Fig. 5. Plane of symmetry

The Wingspan area and the length used is different in different case because of presence of winglet at different angles and thus the wetted area, which is the area that directly comes in the contact of the external airflow, was calculated using the Solidworks. The Equivalent Length, b was calculated using following method as shown in figure 6.

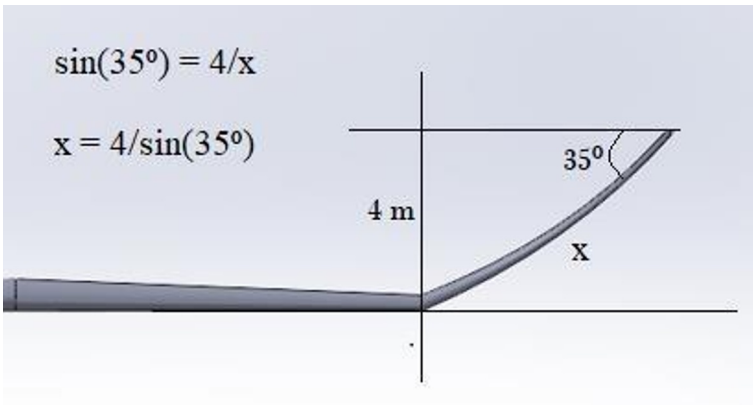

Fig. 6. Calculation of Equivalent Length for the Winglet

$$Equivalent\ Length\ Span, b = Original\ Wingspan + Addition\ because\ of\ winglet \ldots (1)$$

Table 1: The Wetted Area and Equivalent Length for Each Winglet Cant Angle

Winglet Cant Angle	WettedArea, S (sq m.)	EquivalentLength, b (m)
35º	83.52	26.9738
45º	79.98	25.6569
50º	76.47	25.2216
60º	72.25	24.6188
75º	69.12	24.1411
88º	66.25	24.0024
105º	69.12	24.1411

2.2 CFD Simulation Setup

The enclosure with the dimensions as stated in Table 2 was created and the WingletBody was kept in analysis under the enclosure, was then later removed from the enclosure with the Boolean Subtract function. The Enclosure image can be seen in Figure 7.

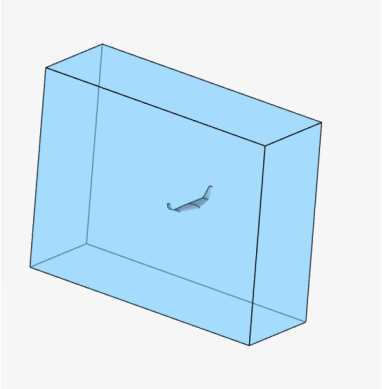

Fig. 7. The Body inside the Enclosure under Translucent View Mode

Table 2: Boundaries of Enclosure

Min	length, m	Max, m	length, m	Equivalent Length, m	Representation
X	-20	X	20	40	From the Left sideto the Right side of the body
Y	-44.75	Y	48.35	93.1	(From The top of the Enclosure untilthe bottom)
Z	-70	Z	50	120	(From the Inlet tothe Outlet)

Incompressible Flow setup with 100 m/s velocity and k-Omega SST Turbulence Modelwas chosen for analysis and Air as flowing medium Following Table 3 shows the properties of Air used at different stage of simulation. Inlet Velocity of 100 m/s and the outlet pressure of 0 Pa is set for simulation. The simulation is done for overall 1000 timesteps.

Table 3: Properties of air used at different Stages of simulation

Altitude (m)	Density (ρ), kg/m^3	Kinematic Viscosity (ν) m^2/s
0	1.1965	0.000015295
10,000	0.4135	0.00003526
15,000	0.1948	0.000073

2.2.1 Meshing

Initially A grid Independence Test was performed for the given simulation setup, and the changing parameter was the fineness of the Mesh Cell (Starting from 1 - 9) where 1 is coarse and 9 is the most finest, then following values of Number of Cells were obtained, as in table 4, where the number of Cells are in Millions and the Drag Coefficient values were observed, and thus looking at figure 8 it was observed that the mesh starts to converge from

number of cells equals to 5.5 Million and so the point after it where the number of cells equal to 6.3 Million was noticed with the drag force value of 0.0278, thus the Setting of Fineness Ratio of 6 was kept for the Entire Simulation Study.

Table 4: Values of Cd for Various Number of Cells

NO.	NO OF CELLS(MILLION)	VALUE OF CD
1	**3.5**	**0.02477**
2	**3.89**	**0.02541**
3	**4**	**0.02683**
4	**4.8**	**0.02906**
5	**5.5**	**0.02805**
6	**6.3**	**0.0278**
7	**7.4**	**0.02766**
8	**8.5**	**0.02765**
9	**9.1**	**0.0277**

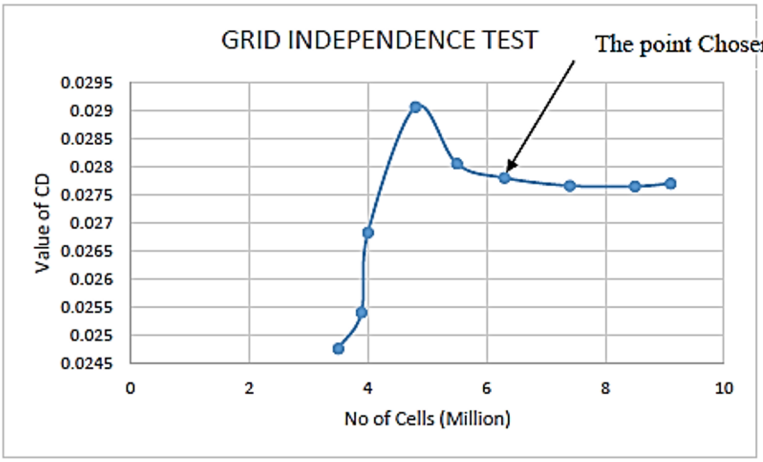

Fig. 8. The Results of Grid Independence Test

The meshing was done with the fineness of 6 with the number of Boundary layer 8 and overall thickness of 0.4 with average growth rate of 1.2. Local Element and Cartesian box Refinements were added to the structure where the meshing size was set to 0.25 m of maximum edge length. Figure 9 shows the meshing of enclosure with the cartesian box and figure 10 and 11 shows the meshed structure of the body followed by Table 5 which the maximum number of nodes in the meshed body.

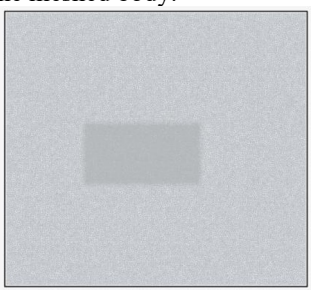

Fig. 9. The overall representation of mesh from the side view with the areain the darker shade with higher number of mesh done by Region Refinement

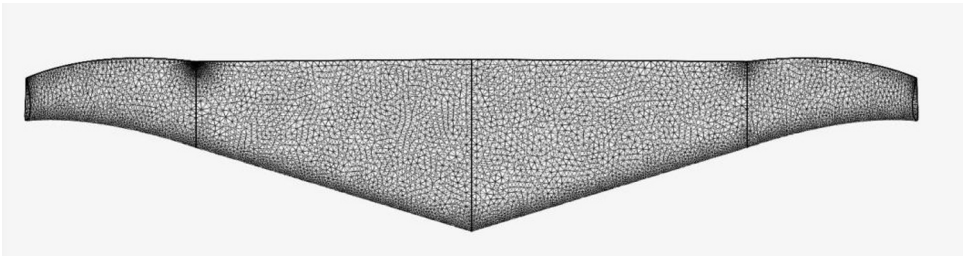

Fig. 10. The Meshed View of the Winglet Body from the top in wireframe structure.

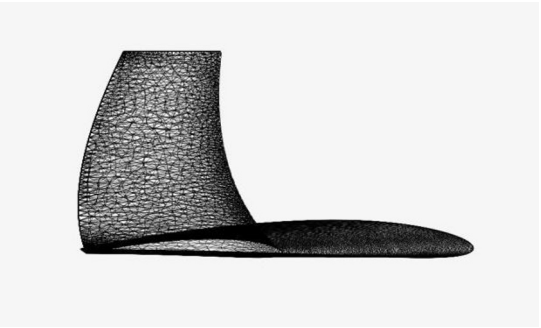

Fig. 11. The Meshed View of the Winglet Body from the side in wireframe structure

Table 5: The Table of Winglet Cant Angle with the respective nodes

Winglet Cant Angle	Number of Nodes
35º	4.3 million
45º	5.6 million
50º	5.7 million
60º	5.3 million
75º	5.6 million
88º	6.5 million
105º	4.5 million

3 Results and Discussion

The entire study is done at the cruising stage, so the angle of attack for all cases is 0º. The main use of winglets is to reduce wake turbulence, which improves fuel efficiency and range. Takeoff and landing are short phases of flight, and the plane spends most of its time cruising. To improve overall fuel efficiency and reduce wake turbulence the study is conducted during the cruising phase of the flight when the angle of attack is 0º. The data which is obtained from the Simulation is then analyzed with three different methods which include

- Comparing the Lift and Drag Coefficients
- Kinematic Turbulence Model
- 2D and 3D Flow Visualization

3.1 Comparing the Lift and Drag Coefficients

The values obtained like this are depicted in the Table 6 at sea level, Ten Thousand meters

and Fifteen Thousand meters, respectively The figure 12(a) shows the lift coefficient against the winglet cant angle and the trend seen is a very straight forward, where the Lift coefficient is maximum at 35º angle and decreases as the winglet angle increases. Thus, it can be said that the Lift Coefficient Graph is inversely proportional to the Cant angle of winglet. The Drag Coefficient Graph (Figure 12(b)) can be said to be parabolic in nature, where it starts decreases a bit then becomes a maximum at 60º cant angle and finally decreasing linearly until 88º. Thus, the aircraft has the lowest Drag coefficient at 45º. Lift Coefficient graph (Figure 12(a)) and the Drag Coefficient Graph(Figure 12(b)) are the graphs which shows at the angle 45º having the second Highest and the lowest value of lift and drag coefficient respectively. So, for the lift to Drag Ratio graph, the highest Lift to Drag Ratio is obtained at 45º and the lowest is obtained at 60º winglet cant angle.

Table 6: The Values of Lift, Drag Coefficient and Lift – to Drag Ratio for Different Altitude of 0m, 10000 m and 15000 m

	AT SEA LEVEL			AT 10000 METERS			AT 15000 METERS		
Winglet Cant Angle, WCA	Lift Coefficient, Cl	Drag Coefficient, Cd	Lift - to - Drag Ratio, L/D Ratio	Lift Coefficient, Cl	Drag Coefficient, Cd	Lift - to - Drag Ratio, L/D Ratio	Lift Coefficient, Cl	Drag Coefficient, Cd	Lift - to - Drag Ratio, L/D Ratio
105	0.8887	0.046	19.3196	0.8921	0.0473	18.8605	0.89	0.045	19.7778
88	0.6478	0.024	26.9917	0.6474	0.0245	26.4245	0.6436	0.0251	25.6414
75	0.6764	0.02788	24.2611	0.673	0.02979	22.5915	0.6742	0.02858	23.5899
60	0.717	0.0398	18.0151	0.7202	0.03974	18.1228	0.7176	0.0396	18.1212
50	0.8872	0.0296	29.973	0.888	0.029	30.6207	0.8616	0.031	27.7936
45	0.8877	0.0278	31.9317	0.8883	0.028	31.725	0.8853	0.02848	31.085
35	0.9191	0.03101	29.6388	0.9185	0.0311	29.5338	0.9136	0.03154	28.9664

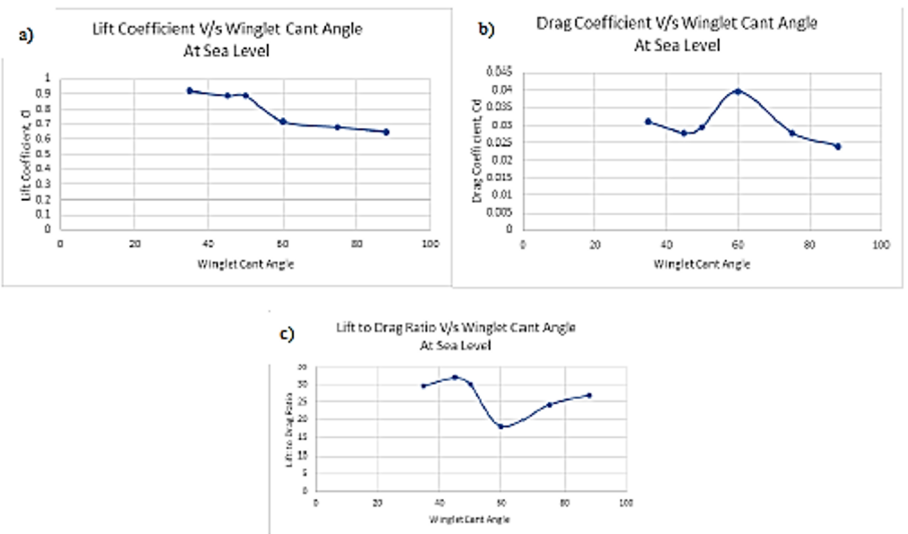

Fig. 12. a) Lift Coefficient V/s Winglet Cant Angle at Sea Level BDrag Coefficient V/s Winglet Cant Angle at Sea Level CLift to Drag Ratio V/s Winglet Cant Angle at Sea Level

Looking at the table 5 it was observed that he obtuse angled winglet of 105 degree has a high lift coefficient (2nd Highest among all) but the drag coefficient is lower is much more

higher in comparison making it the 2nd Lowest Lift To Drag Ratio body followed by 60º winglet. Also, the Obtuse angled Winglet was the only winglet which hadshown an increase in the value of Lift Coefficient as the Height increased, the acute angled ones showed the exact opposite trend.

3.2 Kinematic Turbulence Model

Kinematic turbulent viscosity is the measure of the wake intensity in a given flow field In this case the turbulent Kinematic viscosity has been measured at 20 meters from the Centroid of the wing body at the Tip of the Winglet. The Figure 13 (a) and (b) shows how the Kinematic Turbulent Viscosity is measured and Figure shows the trend Between the Drag Coefficient Cd and The Kinematic Turbulent Viscosity, where the values are obtained from Table 7.

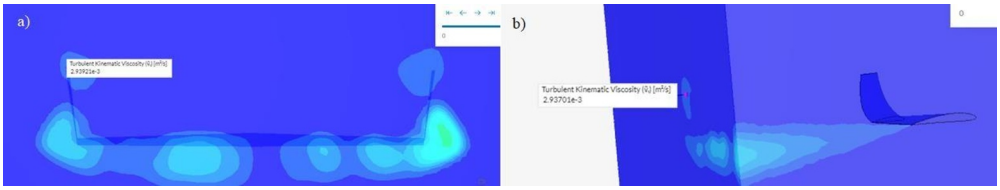

Fig. 13. a) The Turbulent Kinematic Viscosity for 88º winglet at 20 meters from the winglet atthe tip of the winglet b) The Turbulent Kinematic Viscosity for 75º winglet at 20 meters from thewinglet at the tip of the winglet.

Table 7: The Values of Drag Coefficient, Cd and Kinematic Turbulent Viscosity, KTV at Sea Level for Different Cant Angle

Winglet Cant Angle	Drag Coefficient, Cd	Kinematic Turbulent Viscosity, KTV
88	0.024	2.94E-03
75	0.02788	2.93E-03
60	0.0398	7.86E-03
50	0.0296	1.30E-03
45	0.0278	6.15E-04
35	0.03101	1.54E-03

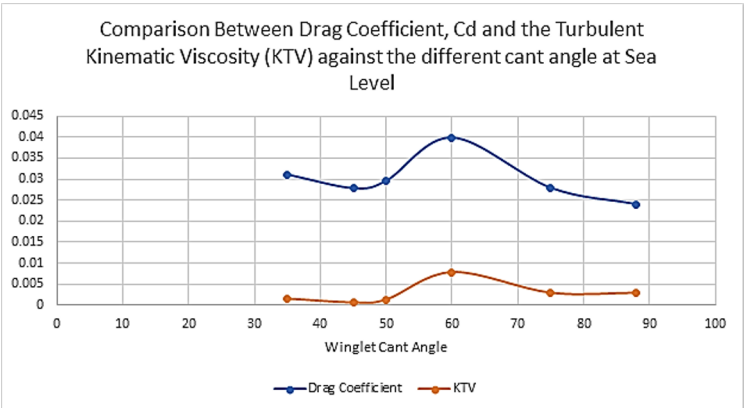

Fig. 14. Comparison Between Drag Coefficient, Cd and the Turbulent Kinematic Viscosity (KTV) against the different cant angle at Sea Level

Therefore, it is seen that the trends for Kinematic Turbulent Viscosity or Wake Turbulence is exactly same as the drag force, where it starts from one point then decreasesto a minimum value after it keeps on increasing until the winglet cant angle of 60º then again decreases in a linear manner, which proves the values of drag coefficient obtained from the CFD simulation are correct in manner.

3.3 2D and 3D Flow Visualization

The Figure 15 (a), (b), (c), (d) shows the Flow Field Visualization in the Terms of Pressure distribution for different Winglet Cant Angles, and the flow visualization also proves the result that was shown by the theoretical Lift and Drag coefficients value. The figure 15(c) shows the smoothest flow distribution where the vortex is generated for the tipof the winglet only thus it has the highest Lift to Drag ratio, whereas for figure 15 (a) double vortex formation occurs one at the tip of wing and the second one at the tip of the winglet, which also proves the point that the Lift to Drag Ratio is among the lowest out of all members. Figure 16 shows the 3D flow visualization the case of 45º Winglet from differentPerspective.

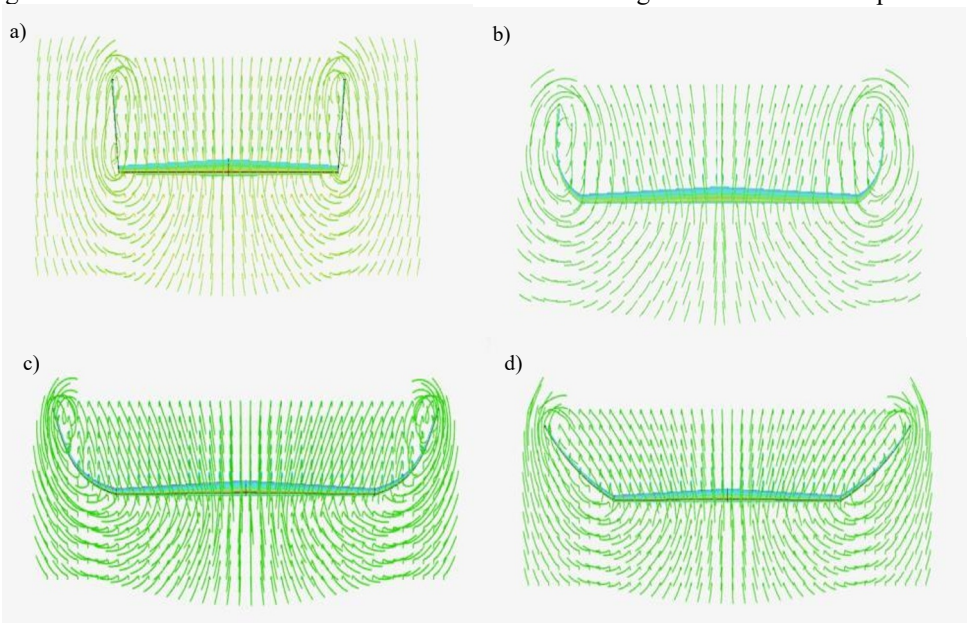

Fig. 15. (a): 2D Pressure Field Visualization for 88º Winglet Cant Angle **(b)**: 2D Pressure Field Visualization for 75º Winglet Cant Angle **(c)**: 2D Pressure Field Visualization for 45º Winglet Cant Angle**(d)**: 2D Pressure Field Visualization for 35º Winglet Cant Angle

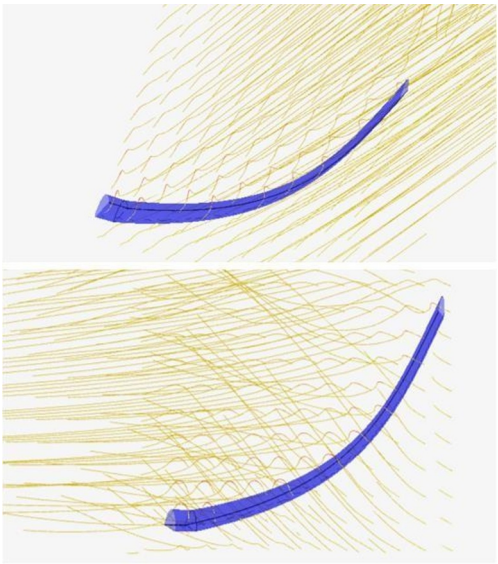

Fig. 16. The Flow Visualization around the 45º Winglet Cant Angle near the winglet area from different point of Reference.

3.4 Crosswind Analysis

The Crosswind analysis was done on the winglet cant angle of 45º and 60º at two different crosswinds conditions:

- Crosswind of 30 m/s acting at an angle 90 Degree from the Actual direction of flow.
- Crosswind of 30 m/s acting at an angle 45 Degree from the Actual Direction of flow.

Since for case 2, equivalent speed in Z direction would be 141.21 m/s, Incompressible flow module cannot be used anymore as the incompressible flow assumption is only valid until 102.9 m/s (Mach 0.3), thus for case two Compressible flow analysis was done.

Table 8: Lift and Drag Coefficient at Different Crosswinds for 45º and 60º

Winglet Cant Angle	Crosswind Angle	Lift Coefficient	Drag Coefficient	Lift to Drag Ratio, L/D Ratio
45º	45º	1.4521	0.0471	30.83
45º	90º	0.7312	0.0272	26.88
60º	45º	1.1617	0.04669	24.88
60º	90º	0.8581	0.0365	23.50

The Lift and Drag coefficient obtained at Sea level when no cross wind was applied were 0.8877 and 0.0278 respectively at 45º Winglet Cant angle. When the crosswind is applied at 45º, the lift coefficient and Drag coefficient increased by 65%, whereas for perpendicular cross wind, the Drag remains the same whereas the lift force reduces by almost 25%. The Lift to drag Ratio is almost the similar for 45º crosswind whereas it has reduced for the 90º crosswind case.

The lift and Drag values obtained for 60º were among the lowest when no crosswind was applied where the lift coefficient was 0.717 and the drag force was 0.0398 with the Lift to Drag ratio merely 18.01. For both the cases of crosswind obtained a much higher lift

coefficient compared to the no crosswind flow, where the lift coefficient was increased by 65%, whereas for the 90º case the lift was reduced again by 25%, the overall lift to drag coefficient did not change too much and nearly same for both the crosswind studies.

4 Conclusion

Winglets are about to finish nearly a century of its invention and 25-30 years of its usage in the everyday planes. The winglets are one of the important parameters in a plane, which helps in the reduction of drag coefficient by a considerable margin which leads to better fuel efficiency and better range for the same aircraft with and without winglets and reduced CO_X and NO_X emissions. This paper aimed to study the effects of variable cant angle in a wing structure which could potentially allow the aircraft to get the overall best performance in improvising the lift to drag ratio overall. The wing studied here, is not an actual wing of any airplane used in commercial aviation sector, but it shows how just by changing the winglet angle, the drag force reduces significantly [6]. The study shows that the 45º winglet cant angle is the best among the other winglet configuration available and the least efficient was the one with winglet angle of 60º. Moreover, for crosswind the lift to drag ratio increases for 60º winglet cant angle whereas it reduces for 45º case. This does not mean that the results obtained are universal, and all the winglets will be having optimum performance at 45º, but it is just a visualization of how for a certain winglet condition how the lift and drag coefficient change. This may be different for different wing, with different size, different aero foil shape, different air conditions, different angle of attack, and various other factors too. The common trend was found that for larger winglet cant angle overall low lift to drag coefficient was noticed, and the flow field was smooth near the tips of winglet where the winglet angle was low. This study did not consider the effects of other winglet design parameters such as winglet sweep angle, winglet toe angle, and winglet taper ratio. But overall, the results obtained from the study were satisfactory in terms of the objectives which were stated were fully achieved. All the calculated parameters show one thing in common that the winglet cant angle have significant impact on the overall efficiency and the Lift to Drag Ratio. Thus, from all the quantitative results obtained, it can be said the controlling the winglet cant angle mid-flight with a device operating on similar mechanism like the elongation of ailerons and changing the rudder angle. When the flight reaches midair, the devices which measure the magnitude of Lift to Drag ratio must be flagged on and it should measure the constant change in Lift to Drag Ratio when the winglet Cant Angle is changed, once the optimum lift to drag ratio is obtained, the flight should continue at the same lift to drag ratio for the rest of the cruising duration. Secondly, a more comprehensive study, which do consider the other winglet parameters like the winglet sweep angle, winglet toe angle, wing and fuselage assembly, must be undertaken in order to fully prove the results generated by this study and from the previous research too.

Acknowledgements

This research was funded by the Universiti Teknologi Malaysia (20J62). Theexperiments were carried out in UTM Aerolab

References

1. Martin, R. (2021, June 30). *Top in-N-out burger execs killed in Calif. plane crash*. IndexArticles. Retrieved June 30, 2022, from https://indexarticles.com/business/nations-restaurant-news/top-in-n-out-burger- execs-

killed-in-calif-plane-crash/ Whitcomb, R.T. *A Design Approach and Selected Wind Tunnel Results at High Subsonic Speeds for Wing-TipMounted Winglets*; Technical Report NASA-TN-D-8260; NASA Langley Research Center: Hampton, VA, USA, 1976.

2. Guerrero, J., Sanguineti, M., & Wittkowski, K. (2018). CFD study of the impact of variable cant angle winglets on total drag reduction. *Aerospace*, Vol *5*(4), 7. https://doi.org/10.3390/aerospace5040126
3. Largeson, G. C. (2001, September 1). *How things work: Winglets*. Smithsonian.com. Retrieved January 27, 2022, from https://www.smithsonianmag.com/air-space-magazine/how-things-work-winglets-2468375/ Maughmer, M., & Kunz, P. (1998). Sailplane winglet design. *TechnicalSoaring*, Vol *22*(4), 116-123.
4. Ujang, M. I., Mat, S., Perumal, K., & Nasir, M. M. (2016, October). Experimentalstudy of UTM-LST generic half model transport aircraft. In *IOP Conference Series: Materials Science and Engineering* (Vol. 152, No. 1, p. 012007). IOP Publishing
5. Slimani, K., Khoulji, S., & Kerkeb, M. L. (2023). Advancements and challenges in energy-efficient 6G mobile communication network. In E3S Web of Conferences (Vol. 412, p. 01036). EDP Sciences.
6. Chandrakasan, B., Subramanian, M., Manoharan, H., Selvarajan, S., & Aluvalu, R. (2023). Future transportation computing model with trifold algorithm for real-time multipath networks. Journal of Autonomous Intelligence, 6(2).